CHEMISTRY
AN ASIAN JOURNAL

DOI: 10.1002/asia.201100489

Construction of Polymer–Protein Bioconjugates with Varying Chain Topologies: Polymer Molecular Weight and Steric Hindrance Effects

Xuejuan Wan,[a] Guoying Zhang,*[a] Zhishen Ge,[a] Ravin Narain,*[b] and Shiyong Liu*[a]

On the occasion of the 10th anniversary of click chemistry

Abstract: We report on the fabrication of well-defined polymer–protein bioconjugates with varying chain architectures, including star polymers, star block copolymers, and heteroarm star copolymers through the specific noncovalent interaction between avidin and biotinylated synthetic polymer precursors. Homopolymer and diblock precursors site-specifically labeled with a single biotin moiety at the chain terminal, chain middle, or diblock junction point were synthesized by a combination of atom-transfer radical polymerization (ATRP) and click reactions. By taking advantage of molecular recognition between avidin and biotin moieties, supramolecular star polymers, star block copolymers, and heteroarm star copolymers were successfully fabricated. This specific binding process was also assessed by using the diffraction optic technology (DOT) technique. We further investigated the effects of polymer molecular weights, location of biotin functionality within the polymer chain, and polymer chain conformations, that is, steric hindrance effects, on the binding numbers of biotinylated polymer chains per avidin within the polymer–protein bioconjugates, which were determined by the standard avidin/2-(4-hydroxyazobenzene)benzoic acid (HABA) assay. The binding numbers vary in the range of 1.9–3.3, depending on the molecular weights, locations of biotin functionality within synthetic polymer precursors, and polymer chain conformations.

Keywords: bioconjugates · click chemistry · polymers · steric hindrance · supramolecular chemistry

Introduction

The covalent or noncovalent attachment of synthetic polymer chains onto proteins or other biomacromolecules can endow them with improved solubility and stability, increased plasma half-lives and bioavailability, and reduced immunogenicity. Biohybrid polymers and their self-assembled nanostructures have found broad applications in biomedical and biotechnology fields, such as delivery of protein and gene therapeutics, enzyme catalysis, tissue engineering, bionanoreactors, and artificial enzymes or cells.[1] Concerning their synthesis, two main types of design strategies have been developed. The conventional one relies on the covalent or noncovalent conjugation of synthetic polymer precursors onto biomacromolecules, such as proteins. In the covalent approach, quantitative, highly efficient coupling reactions, such as amidation reactions between activated esters and amine functionalities,[2] thiol–ene[3] and azide–alkyne 1,3-dipolar cycloaddition click reactions,[4] and thiol/pyridyl disulfide exchange reactions,[5] have been frequently utilized to fabricate well-defined hybrid bioconjugates. As for the noncovalent approach, biotin/avidin,[6] cofactor/apoprotein reconstitution,[7] saccharide/concanavalin A,[8] and other specific host–guest molecular recognition processes[9] have been employed. The second type of strategy relies on the use of well-developed controlled/living polymerization techniques,[10] such as atom-transfer radical polymerization (ATRP) and reversible addition–fragmentation chain transfer (RAFT) polymerization, which allow for the direct preparation of well-defined polymer–protein conjugates from protein-based ATRP initiators[11] and macroRAFT agents.[12]

[a] Dr. X. Wan, Prof. G. Zhang, Prof. Z. Ge, Prof. S. Liu
CAS Key Laboratory of Soft Matter Chemistry
Hefei National Laboratory for Physical Sciences at the Microscale
Department of Polymer Science and Engineering
University of Science and Technology of China
Hefei, Anhui 230026 (P.R. China)
Fax: (+86) 551-360-7348
E-mail: sliu@ustc.edu.cn
gyzhang@ustc.edu.cn

[b] Prof. R. Narain
Department of Chemical and Materials Engineering
University of Alberta
Edmonton, Alberta T6G 2G6 (Canada)
Fax: (+1) 780-492-2881
E-mail: narain@ualberta.ca

Supporting information for this article is available on the WWW under http://dx.doi.org/10.1002/asia.201100489.

Of the above approaches, the strong, specific, noncovalent interaction between avidin and biotin, upon appropriate functionalization with a synthetic polymer chain segment, was often employed to construct supramolecular synthetic polymer–protein hybrid bioconjugates.[13] Compared with the covalent approach, noncovalent ones are less disruptive to the native protein conformation and relevant biological activities. Avidin contains four binding sites for biotin, and the biotin/avidin pair possesses a high binding affinity with K_d values up to 10^{-15} M. However, it has been reported that biotinylated polymers, depending on their molecular weight (MW) and chain topology, typically possess decreased affinity for avidin. Previously, Maynard et al. reported the fabrication of polymer/avidin bioconjugates by either direct ATRP from avidin-based initiators or noncovalent conjugation between avidin and biotinylated poly(*N*-isopropylacrylamide) (PNIPAM).[14] In the latter case, the binding number of PNIPAM chain per avidin was quantified to be 3.6; thus, supramolecular star polymers possessing an avidin core and about three to four PNIPAM arms were prepared. Haddleton et al. and Frey et al. fabricated poly(amidoamine) (PAMAM) dendrimer and linear-dendritic diblock copolymers with a biotin functionality attached at the dendrimer focal point or the linear chain terminal, respectively.[15] Their subsequent conjugation with avidin afforded star polymer bioconjugates, as evidenced by the standard 2-(4-hydroxyazobenzene)benzoic acid (HABA)/avidin assay. In both cases, the actual binding numbers of dendritic or linear-dendritic arms per avidin were not discussed. In 1997, Gruber et al. reported the conjugation of biotinylated polyethylene glycol (PEG) with avidin, and the effects of PEG chain length and end-group modification with hydrophobic dyes or other functionalities on the time-dependent structural evolution of as-prepared bioconjugates.[16] Recently, Kwon et al. reported that the binding numbers of biotinylated PEG/avidin conjugates are highly dependent on the PEG chain length, which decreased from about four to one when the PEG MW increased from 588 to 5000 Da.[17]

In addition to the above-described MW effects of biotinylated polymers on their noncovalent conjugation with avidin, the location of biotin functionality within the polymer precursor (chain terminal or chain middle) might also play crucial roles. Based on chemical intuition, precursors with the biotin moiety attached at the chain middle should suffer from increased steric hindrance during their conjugation with avidin. However, this aspect has been far less explored and no quantitative data were presented in relevant literature reports. It is thus highly desirable to quantitatively determine the binding numbers and systematically investigate the effects of MW and chemical structures of biotinylated polymers on the formation of hybrid bioconjugates. Moreover, previous reports in this area have focused on the fabrication of synthetic polymer/avidin bioconjugates with a star-type topology by employing biotin-terminated linear polymers and dendrimers. By appropriately designing the chemical structures of biotinylated polymers, hybrid bioconjugates with other chain topologies, such as star block copolymers and heteroarm star copolymers, can also be fabricated.

Herein, we report on the fabrication of well-defined polymer–protein bioconjugates with varying chain architectures, including star polymers, star block copolymers, and heteroarm star copolymers, through the specific noncovalent interaction between avidin and biotinylated synthetic polymer precursors. Homopolymer and diblock precursors site-specifically labeled with one single biotin moiety at the chain terminal, chain middle, or diblock junction point were synthesized by a combination of ATRP and click reactions (Scheme 1). By taking advantage of the specific molecular recognition between avidin and biotin moieties, supramolecular star polymers, star block copolymers, and heteroarm star copolymers were successfully fabricated (Scheme 2). Most importantly, the effects of polymer MW and the location of the biotin functionality within polymer chains, that is, steric hindrance effects, on their binding affinity with avidin and the binding numbers (e.g., number of noncovalently grafted polymer arms) were further quantitatively determined by the standard avidin/HABA assay.

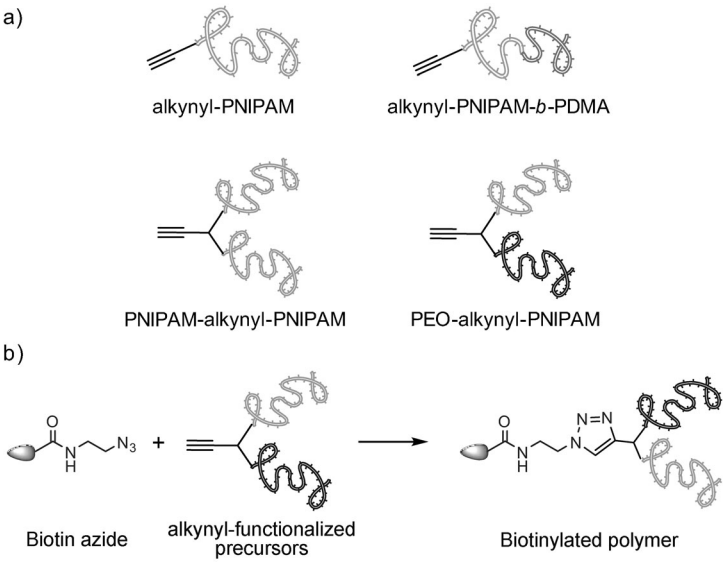

Scheme 1. Schematic illustration of a) the synthesis of homopolymers and diblock copolymers with one single alkynyl functionality at different locations (chain terminal, chain middle, and diblock junction point), and b) click synthesis of water-soluble thermoresponsive homopolymers and diblock copolymers site-specifically labeled with biotin functionality. PDMA = poly(*N*,*N*-dimethylacrylamide).

Experimental Section

Materials

N-Isopropylacrylamide (NIPAM; TCI) was recrystallized twice from benzene/hexane (2:1 v/v) prior to use. *N*,*N*-Dimethylacrylamide (DMA; TCI) was vacuum distilled from calcium hydride and stored at −15 °C prior to use. 1,1′-Carbonyldiimidazole (CDI), *N*,*N*,*N*′,*N*″,*N*″-pentamethyldiethylenetriamine (PMDETA), 2-chloropropionyl chloride, CuCl, CuBr,

CHEMISTRY
AN ASIAN JOURNAL

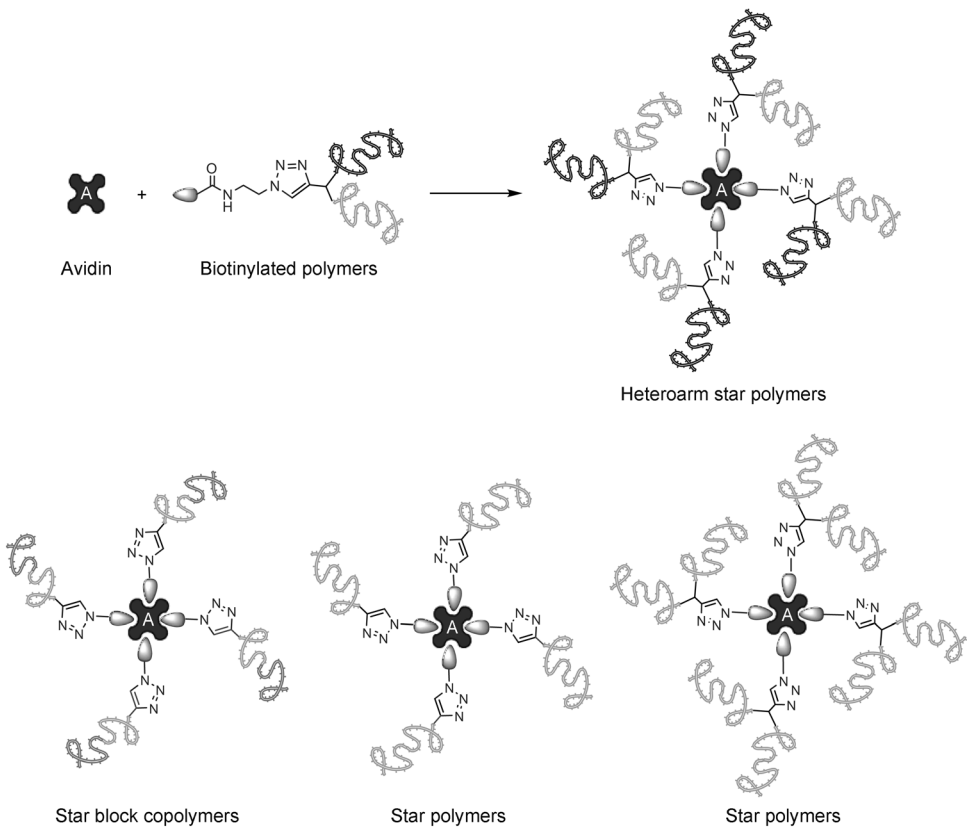

Scheme 2. Schematic illustration of the fabrication of polymer–protein bioconjugates with varying chain topologies (star polymers, star block copolymers, and heteroarm star copolymers) through specific noncovalent interactions between avidin and synthetic homopolymer and diblock copolymers site-specifically labeled with one single biotin functionality.

2,2-bis(hydroxymethyl)propionic acid (bis-MPA), propargyl alcohol, biotin, and avidin were purchased from Aldrich and used as received. All other reagents were purchased from Shanghai Chemical Reagent Co. and used as received. HABA/avidin reagent (lyophilized powder) was purchased from Sigma and used according to standard procedures. 1-Azido-3-aminopropane,[18] tris[2-(dimethylamino)ethyl]amine (Me_6TREN),[19] alkynyl-functionalized resin (alkynyl-resin),[20] azide-terminated poly(ethylene oxide) monomethyl ether (PEO-N_3),[21] ATRP initiators, including propargyl 2-chloropropionate[22] and alkynyl-Cl_2,[23] and methyl 3,5-bis(-propargyloxy)benzyl alcohol (alkynyl-OH-alkynyl),[20] were synthesized according to literature procedures (Scheme 3). Water was deionized with a Milli-Q SP reagent water system (Millipore) to a specific resistivity of 18.4 $M\Omega\,cm^{-1}$.

Sample Preparation

General approaches employed for the synthesis of biotinylated polymer precursors and polymer–protein bioconjugates with varying chain architectures (star polymers, star block copolymers, and heteroarm star polymers) through specific noncovalent interactions between avidin and biotin moieties within polymer precursors are shown in Schemes 1–3.

Synthesis of Azide-Functionalized Biotin (Biotin Azide) (Scheme 3a)

Biotin azide was synthesized by the CDI-mediated esterification reaction. Biotin (0.61 g, 2.5 mmol) was first dissolved in *N,N*-dimethylformamide (DMF; 15 mL) at 55 °C. After cooling to room temperature, CDI (0.73 g, 4.5 mmol) in DMF (3 mL) was slowly added and the reaction mixture was allowed to stir for 3 h at room temperature. Subsequently, 1-azido-3-aminopropane (0.75 g, 7.5 mmol) in DMF (6 mL) was added dropwise over about 0.5 h and the reaction mixture was left stirring for another 12 h. The solvent was then removed in vacuo and the residues were purified by recrystallization in a mixture of 1-butanol/acetic acid/water (70:7:10, v/v/v). The obtained white solid was washed with diethyl ether three times and dried in a vacuum oven to afford biotin azide (0.74 g, 90.7 %). ^{1}H NMR (CD_3OD, Figure 1a): $\delta = 4.50$ (m, 1H; $-S-CH_2-CH-$), 4.33 (m, 1H; $-S-CH-CH-$), 3.38 (m, 4H; $-CH_2CH_2CH_2N_3$), 3.22 (m, 1H; $-S-CH-CH-$), 2.93, 2.72 (t, 2H; $-S-CH_2-CH-$), 2.19 (t, 2H; $-CH_2CONHCH_2$), 1.54–1.83 (m, 6H; $-CH_2CH_2CH_2CH_2CO-$), 1.44 ppm (m, 2H; $-CH_2CH_2CH_2N_3$).

Synthesis of Alkynyl-PNIPAM, Alkynyl-PNIPAM-b-PDMA, and Alkynyl-$(PNIPAM)_2$ (Scheme 3b and c)

Alkynyl-PNIPAM, alkynyl-PNIPAM-*b*-PDMA, and alkynyl-$(PNIPAM)_2$ were prepared by the ATRP or consecutive ATRP techniques in isopropanol using propargyl 2-chloropropionate (for alkynyl-PNIPAM and alkynyl-PNIPAM-b-PDMA diblock) and alkynyl-Cl_2 (for alkynyl-$(PNIPAM)_2$) as the initiators, according to well-established literature procedures.[24] Structural parameters were characterized by ^{1}H NMR spectroscopy and gel permeation chromatography (GPC) and the results are listed in Table 1.

Synthesis of PEO-Alkynyl-PNIPAM Diblock Copolymer Bearing One Alkynyl Functionality at the Junction Point (Scheme 3d)

PEO-OH-alkynyl was prepared by the click reaction of PEO-N_3 with an excess of alkynyl-OH-alkynyl. PEO_{45}-N_3 (1.0 g, 0.5 mmol N_3 moieties), alkynyl-OH-alkynyl (2.16 g, 10 mmol), and PMDETA (0.1 g, 0.6 mmol) were dissolved in DMF (100 mL) in a Schlenk flask. The flask was subjected to three freeze/pump/thaw cycles and CuBr (72 mg, 0.5 mmol) was then introduced under the protection of an N_2 atmosphere. After one ad-

Table 1. Structural parameters of alkynyl-functionalized polymer precursors with varying chain topologies, as shown in Scheme 1.

Samples	$M_{n,NMR}$[a]	M_n[b]	M_w/M_n[b]	DP[a]		
				PNIPAM	PDMA	PEO
alkynyl-$PNIPAM_{19}$	2300	3100	1.07	19	–	–
alkynyl-$PNIPAM_{50}$	5800	6900	1.08	50	–	–
alkynyl-$PNIPAM_{19}$-$PDMA_8$	2900	4200	1.09	19	8	–
alkynyl-$PNIPAM_{69}$-$PDMA_{65}$	14400	13300	1.09	69	65	–
$PNIPAM_{27}$-alkynyl-$PNIPAM_{27}$	6500	6200	1.07	27	–	–
PEO_{45}-alkynyl-$PNIPAM_{15}$	4400	6100	1.07	15	–	45
PEO_{45}-alkynyl-$PNIPAM_{45}$	7500	8300	1.10	45	–	45

[a] Determined by ^{1}H NMR spectroscopy in $CDCl_3$. DP = degree of polymerization. [b] Determined by GPC using DMF as the eluent.

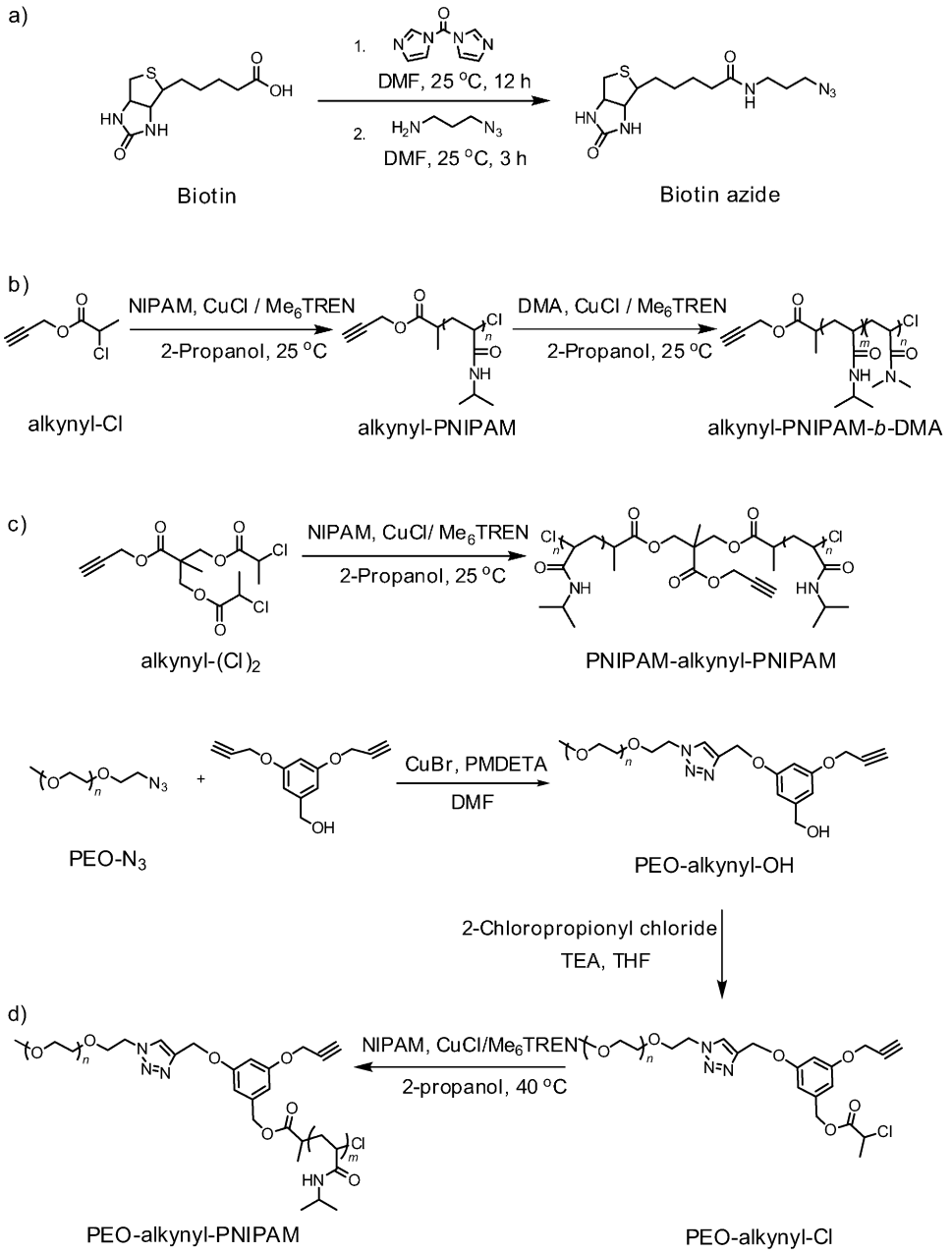

Scheme 3. Schematic illustration of the synthesis of a) biotin azide and alkynyl-functionalized precursors: b) alkynyl-PNIPAM and alkynyl-PNIPAM-*b*-PDMA, c) PNIPAM-alkynyl-PNIPAM, and d) PEO-alkynyl-PNIPAM. DMF = *N*,*N*-dimethylformamide, TEA = triethylamine, THF = tetrahydrofuran.

ditional freeze/pump/thaw cycle, the click reaction was carried out at 80 °C for 4 h under the protection of N_2. After removing all of the solvents under reduced pressure, the reaction mixture was then dissolved in CH_2Cl_2 and passed through a neutral alumina column to remove the catalyst. The elution was concentrated on a rotary evaporator and the crude product was obtained by precipitation into an excess of ethyl ether. The above dissolution/precipitation cycle was repeated three times. The collected white solid was washed and dried in a vacuum oven at room temperature to give a constant weight (0.82 g, 74.0 % yield; $M_n = 2\,200$, $M_w/M_n = 1.09$).

PEO-OH-alkynyl (0.60 g, 0.27 mmol OH functionality), TEA (50 mg, 0.5 mmol), and anhydrous THF (20 mL) were added to a 100 mL dry round-bottomed flask. The flask was immersed in an ice water bath for 10 min and a solution of 2-chloropropionyl chloride (51 μL, 0.5 mmol) in anhydrous THF (5 mL) was then added dropwise by a dropping funnel over 30 min under vigorous stirring. The reaction mixture was stirred in an ice water bath for 1 h and then at room temperature overnight. The insoluble salts were then filtered off and all the solvents were removed by rotary evaporation. The crude product was dissolved in CH_2Cl_2 and precipitated into excess diethyl ether. This dissolution/precipitation cycle was repeated twice. After drying in a vacuum oven at room temperature to give a constant weight, PEO-alkynyl-Cl was obtained as a white powder (0.45 g, 62.4 % yield; $M_n = 2\,300$, $M_w/M_n = 1.08$).

PEO-alkynyl-PNIPAM was synthesized by ATRP of NIPAM monomer using PEO-alkynyl-Cl as the initiator following well-established literature procedures, and the structural parameters of PEO-alkynyl-PNIPAM precursors are summarized in Table 1.

Synthesis of Biotinylated Polymers (Scheme 1)

Typical procedures are described as follows: Biotin azide (0.06 mmol), alkynyl-functionalized polymer precursor (0.05 mmol alkynyl moieties), and PMDETA (0.06 mmol) were dissolved in DMF (20 mL) in a Schlenk flask. After the flask was subjected to three freeze/pump/thaw cycles, CuBr (0.06 mmol) was introduced under the protection of an N_2 atmosphere. The reaction mixture was allowed to stir overnight at room temperature under the protection of N_2. Alkynyl-functionalized resin (70 mg, ≈0.1 mmol alkynyl moieties) was added and the reaction mixture was left stirring under the protection of N_2 for another 4 h. After filtering off the resins, the filtrate was evaporated to dryness under reduced pressure. The residues were dissolved in CH_2Cl_2 and passed through a neutral alumina column to remove the catalyst. The final product was dried in vacuo to give a constant weight at room temperature. The structural parameters of all biotinylated polymers (biotin-PNIPAM, biotin-PNIPAM-*b*-PDMA, PNIPAM-biotin-PNIPAM, and PEO-biotin-PNIPAM) with varying MW and chain architectures were characterized by ^{1}H NMR spectroscopy and GPC, and the results are shown in Table 2.

HABA/Avidin Assay

The HABA/avidin reagent purchased from Sigma was reconstituted with deionized water (10 mL) in a glass vial that contained 0.3 mM HABA, avidin (0.45 g L^{-1}, 6.6×10^{-6} mol L^{-1}), and buffering salts at pH ≈ 7.3. In a quartz cuvette containing 900 μL of the above-prepared HABA/avidin assay solution, the optical absorbance at 500 nm ($A_{HABA/avidin}$) was recorded. Then, an aqueous solution of biotinylated polymers (biotin-PNIPAM, biotin-PNIPAM-*b*-PDMA, PNIPAM-biotin-PNIPAM, or PEO-biotin-

Table 2. Structural parameters of biotinylated polymers and average binding numbers of biotinylated polymer chains per avidin.

Samples	M_n[a]	M_n[b]	M_w/M_n[b]	Binding numbers[c]
biotin-PNIPAM$_{19}$	2600	3500	1.06	3.3
biotin-PNIPAM$_{50}$	6100	7400	1.08	2.9
biotin-PNIPAM$_{19}$-*b*-PDMA$_8$	3200	4700	1.08	2.9
biotin-PNIPAM$_{69}$-*b*-PDMA$_{65}$	14700	13800	1.06	1.9
PNIPAM$_{27}$-biotin-PNIPAM$_{27}$	6800	6400	1.05	1.9
PEO$_{45}$-biotin-PNIPAM$_{15}$	4700	6300	1.07	2.5
PEO$_{45}$-biotin-PNIPAM$_{45}$	7800	8500	1.08	2.2

[a] Determined by ^{1}H NMR spectroscopy in $CDCl_3$ or [D$_4$]MeOH. [b] Determined by GPC using DMF as the eluent. [c] Binding numbers of biotinylated polymer chains per avidin as determined by the standard HABA/avidin assay.

PNIPAM with varying chain lengths and block length ratios) at a predetermined concentration was added in a batch to the cuvette and the absorbance at 500 nm ($A_{HABA/avidin+sample}$) was then recorded. The binding numbers of biotinylated polymer chains per avidin were calculated by using Equations (1)–(2, and 3):

$$\Delta A_{500nm} = \alpha A_{HABA/avidin} - A_{HABA/avidin+sample} \quad (1)$$

in which α is the dilution factor of HABA/avidin assay solution upon the addition of aqueous solution of biotinylated polymer).

$$\mu mol\ biotin/mL = (\Delta A_{500nm}/34)/\beta \quad (2)$$

in which the mM extinction coefficient at 500 nm is 34 and β is dilution factor of biotinylated polymer aqueous solution after addition into the cuvette).

$$\text{binding number (mole biotin/mole avidin)} = \frac{\mu mol\ biotin/mL\ sample}{\mu mol\ avidin/mL\ sample} \quad (3)$$

Characterization

^{1}H NMR spectra were measured on a Bruker 300 MHz spectrometer using CD_3OD or $CDCl_3$ as solvents. MWs and MW distributions were determined by a GPC equipped with a Waters 1515 pump and a Waters 2414 differential refractive index detector (set at 30 °C). It used a series of three linear Styragel columns (HT2, HT4, and HT5) at an oven temperature of 45 °C. The eluent was DMF at a flow rate of 1.0 mL min^{-1}. FTIR spectra were measured on a Bruker Vector 22 Fourier transform infrared spectrometer using the KBr disk method. UV/Vis spectra were recorded on a Unico UV-2102 PC spectrophotometer. Matrix-assisted laser desorption/ionization time-of-flight mass spectrometry (MALDI-TOF MS) were recorded in the linear mode on a Bruker BIFLEXe III using a nitrogen laser (337 nm) and an accelerating potential of 20 kV. 2,5-Dihydroxybenzoic acid (DHB; Aldrich) was used as the matrix and $NaBF_4$ was added to improve ionization. For diffractive optics technology (DOT) measurements, dotLab data were recorded on a DOT system from Axela Biosensors; the sensor chip was composed of polystyrene as the substrate and avidin groups were attached on the surface. Phosphate buffered saline (PBS) was used as the eluent. Aqueous solutions of biotinylated polymers were loaded into the sensor chip according to the designed program. The binding events were taking place on the surface of the sensor chip by avidin–biotin interactions and the height of the diffractive pattern was increased. The increase in signals was detected synchronously by using a laser-based optical system, and the real-time data generated were presented in dotLab software.

Results and Discussion

Each avidin molecule contains a maximum of four biotin binding sites with a high binding constant ($K_d \approx 10^{-15}$ M) and this property has successfully utilized for the construction of polymer/avidin bioconjugates.[6] However, the determination of actual structural information of as-prepared hybrid bioconjugates relies on the quantification of binding numbers and the understanding of effects of polymer MW and location of biotin moieties within the polymer on the binding affinity. In the current work, a series of biotinylated homopolymers and diblock copolymers with varying chain architecture and chain lengths were synthesized, and the location of biotin within the synthetic polymer chains ranges from the chain terminal to the chain middle and diblock junction point (Scheme 2). Taking advantage of the special interaction between avidin and the biotin moiety, we fabricated bioconjugates with varying star-type topologies, including star polymers, star block copolymers, and heteroarm star polymers (Scheme 3). We further quantified the binding numbers (i.e., number of grafted polymer chains per star-type bioconjugate) of biotinylated polymer chains by the standard HABA/avidin assay and explored the effects of polymer MW and biotin location within the polymer chain, that is, steric hindrance effects, on the formation of polymer–protein hybrid bioconjugates.

Synthesis of Biotinylated Polymers of Varying MWs and Chain Architectures

Biotin azide was synthesized by the amidation reaction of biotin with 1-azido-3-aminopropane (Scheme 3a). Previously, Hsu et al. reported the synthesis of biotin azide by utilizing *o*-(benzotriazol-1-yl)-*N,N,N′,N′*-tetramethyluronium hexafluorophosphate (HBTU) as the catalyst, but the yield was only about 40% after purification.[25] We slightly modified the experimental procedures by activating biotin with CDI for 3 hours and the yield dramatically increased to 90.7%. The ^{1}H NMR spectrum of biotin azide is shown in Figure 1a and the signal integral ratios confirmed the successful preparation of biotin azide.

The alkynyl-terminated precursor, alkynyl-PNIPAM, was synthesized by ATRP of NIPAM monomer by using propargyl 2-chloropropionate and CuCl/Me$_6$TREN as initiator and catalyst, respectively (Scheme 3b). This polymerization system is successful and efficient for the NIPAM monomer and the DP can be facilely adjusted by the monomer/initiator feed monomer ratio and monomer conversion.[22] The ^{1}H NMR spectrum of alkynyl-PNIPAM is shown in Figure 1b. Resonance signals at $\delta = 4.7$ ppm (signal *a*) are ascribed to methylene protons of the terminal propargyl group and signals at $\delta = 3.9$–4.1 ppm (signal *d*) are assigned to the methenyl proton adjacent to amide residues in the PNIPAM segment. On the basis of the integral ratio of sig-

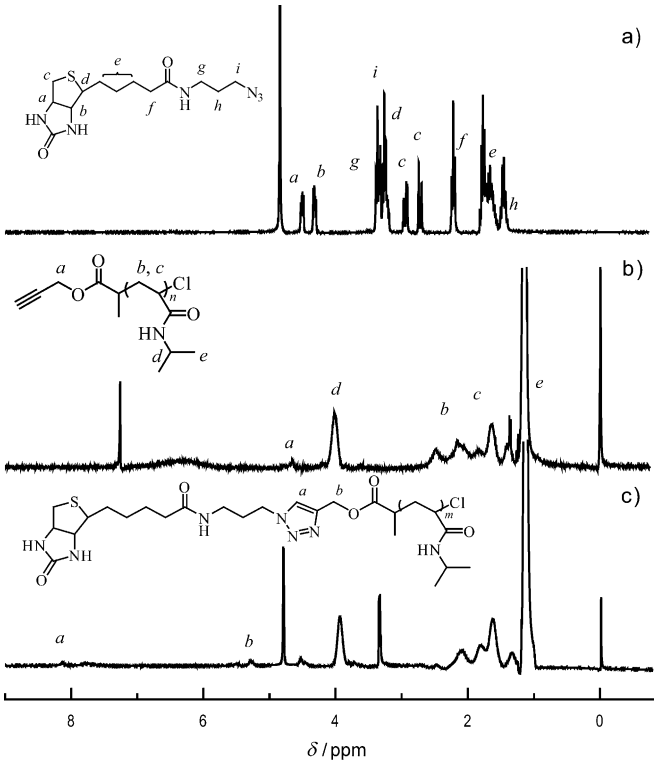

Figure 1. ^{1}H NMR spectra recorded for a) biotin azide in [D$_4$]MeOH, b) alkynyl-PNIPAM$_{19}$ in CDCl$_3$, and c) biotin-PNIPAM$_{19}$ in [D$_4$]MeOH.

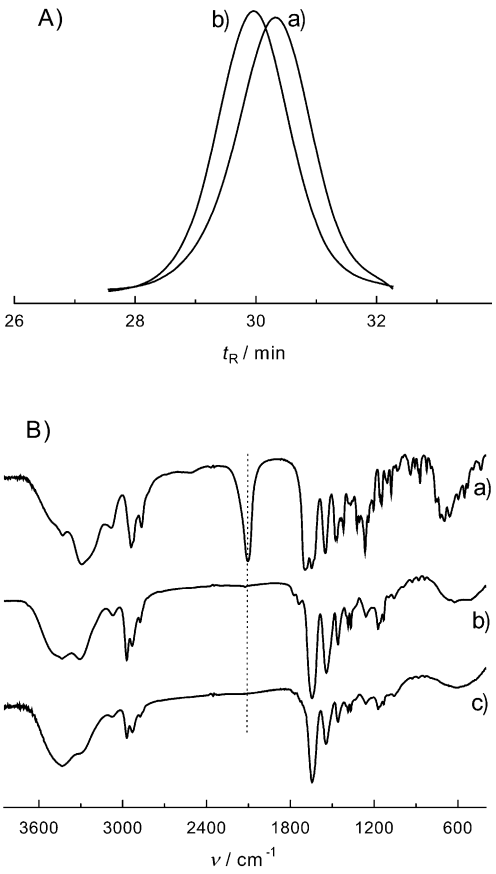

Figure 2. A) GPC traces in DMF obtained for a) alkynyl-PNIPAM$_{19}$ and b) biotin-PNIPAM$_{19}$. B) FTIR spectra obtained for a) biotin azide, b) alkynyl-PNIPAM$_{19}$, and c) biotin-PNIPAM$_{19}$.

nals *a* to *d*, the DP of alkynyl-PNIPAM was determined to be 19, thus the polymer was denoted as alkynyl-PNIPAM$_{19}$. The GPC trace of the alkynyl-PNIPAM$_{19}$ precursor in DMF is shown in Figure 2 A, which reveals a relatively sharp and symmetric elution peak with no tailing or shoulder at lower or higher MWs, thus indicating that the ATRP process was conducted in a controlled manner. The MALDI-TOF mass spectrum of alkynyl-PNIPAM$_{19}$ reveals an envelope of signals extending from 1000 to 4000 Da with an $M_{n,MALDI}$ of 2300 Da and an M_w/M_n of 1.07 (Figure 3 a), which is in good agreement with ^{1}H NMR spectroscopy results (Figure 1 b).

Previously, biotin-terminated PNIPAM was synthesized by a controlled radical polymerization technique starting from biotin-based initiators.[14b] In the current work, we employed the click reaction. Upon reacting with an excess of biotin azide through the click reaction, the chain end of alkynyl-PNIPAM$_{19}$ was functionalized with biotin and this process afforded biotin-PNIPAM$_{19}$ (Scheme 3 b). The unreacted biotin azide residues were eliminated by treatment with alkynyl-functionalized resin through click grafting followed by simple filtration procedures. The ^{1}H NMR spectrum of biotin-PNIPAM$_{19}$ is shown in Figure 1 c. Resonance signals ascribed to the propargyl group shifted from $\delta = 4.7$ (signal *a*, Figure 1 b) to 5.2 ppm (signal *b*, Figure 1 c), and a new resonance signal appeared at $\delta = 8.14$ ppm, which is characteristic of the formation of 1,2,3-triazole rings. In addition, the GPC curve of biotin-PNIPAM$_{19}$ exhibited a discernible shift towards higher MW (Figure 2 A), and the elution profile was again monomodal and quite symmetric, thereby implying that the click reaction went to completion with high efficiency. The MALDI-TOF mass spectrum of biotin-PNIPAM$_{19}$ presents a series of signals with the highest intensity located at *m*/*z* 2605.2 (Figure 3 b). Compared with that of the alkynyl-PNIPAM$_{19}$ precursor, a clear and systematic shift in the MW distribution was observed. For biotin-PNIPAM$_{19}$, MALDI-TOF MS analysis gave an $M_{n,MALDI}$ of 2600 Da and an M_w/M_n of 1.09. These results confirmed the successful preparation of biotin-PNIPAM$_{19}$. Moreover, FTIR absorbance peaks characteristic of azide and alkynyl moieties within biotin azide and alkynyl-PNIPAM$_{19}$, respectively, at 2100 cm^{-1} completely disappeared after the click reaction (Figure 2 B), suggesting excess biotin azide was completely removed. By following similar procedures, biotin-PNIPAM$_{50}$ with an $M_{n,GPC}$ of 7400 Da and an M_w/M_n of 1.08 was also synthesized. Structural parameters are summarized in Table 2.

For the synthesis of biotin-terminated diblock copolymer, biotin-PNIPAM-*b*-PDMA, the alkynyl-terminated precursor alkynyl-PNIPAM-*b*-PDMA was synthesized first by ATRP of the DMA monomer by utilizing alkynyl-PNIPAM$_{19}$ as the macroinitiator (Scheme 3 b). The ^{1}H NMR spectrum and the associated signal assignments of alkynyl-PNIPAM-*b*-PDMA

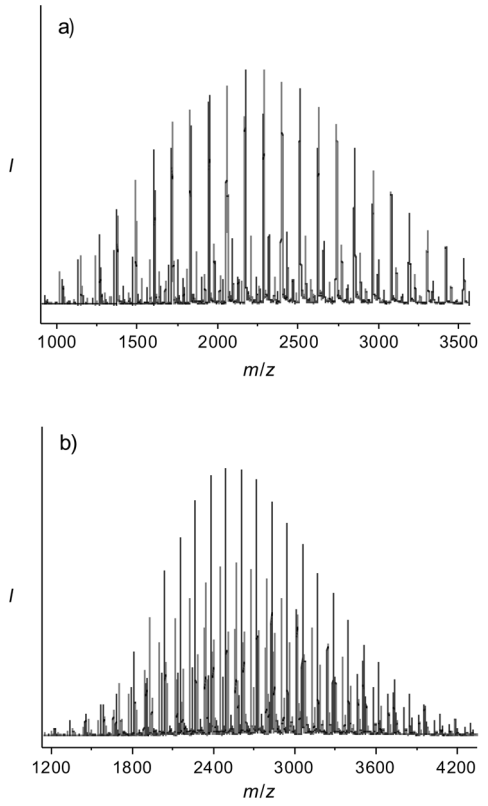

Figure 3. MALDI-TOF mass spectra recorded for a) alkynyl-$PNIPAM_{19}$ and b) biotin-$PNIPAM_{19}$.

are shown in Figure S1a in the Supporting Information. On the basis of signal integral ratios, the DP of the PDMA block was determined to be eight, thus the diblock copolymer was denoted as alkynyl-$PNIPAM_{19}$-*b*-$PDMA_8$. The GPC trace of alkynyl-$PNIPAM_{19}$-*b*-$PDMA_8$ exhibited a clear shift towards higher MW relative to that of alkynyl-$PNIPAM_{19}$, and the peak is reasonably symmetric without any tailing, indicating a successful chain extension of the PDMA block (Figure S2 in the Supporting Information).

Subsequently, biotin-$PNIPAM_{19}$-*b*-$PDMA_8$ was synthesized by the click reaction of biotin azide with alkynyl-$PNIPAM_{19}$-*b*-$PDMA_8$ by following similar procedures as those employed for the preparation of biotin-$PNIPAM_{19}$. Resonance signals ascribed to biotin azide can be clearly seen in the NMR spectrum of alkynyl-$PNIPAM_{19}$-*b*-$PDMA_8$ (Figure S1b in the Supporting Information). Compared with the alkynyl-$PNIPAM_{19}$-*b*-$PDMA_8$ precursor, a new resonance signal appeared at $\delta = 8.10$ ppm, which was characteristic of the formation of 1,2,3-triazole linkages; this again implied the successful synthesis of biotin-$PNIPAM_{19}$-*b*-$PDMA_8$. Compared with that of alkynyl-$PNIPAM_{19}$-*b*-$PDMA_8$, the GPC trace of biotin-$PNIPAM_{19}$-*b*-$PDMA_8$ in DMF exhibited a slight shift towards higher MW (Figure S2 in the Supporting Information). In addition, the GPC trace was also monomodal and quite symmetric, suggesting that the click reaction did not affect the structural integrity. For comparison, and the investigation into MW effects on the binding affinity between avidin and biotinylated polymers, biotin-$PNIPAM_{50}$ with an $M_{n,GPC}$ of 7400 Da and M_w/M_n of 1.08, and biotin-$PNIPAM_{69}$-*b*-$PDMA_{65}$ with an $M_{n,GPC}$ of 13800 Da and M_w/M_n of 1.06 were also synthesized. Their structural parameters are summarized in Table 2.

Note that in the above-prepared biotin-PNIPAM and biotin-PNIPAM-*b*-PDMA, the biotin functionality was located at the chain terminal of the PNIPAM homopolymer and PNIPAM-*b*-PDMA diblock copolymer. We further prepared PNIPAM-biotin-PNIPAM and PEO-biotin-PNIPAM in which the biotin moiety was located at the chain middle of the PNIPAM homopolymer and the diblock junction point, respectively. For the synthesis of PNIPAM-biotin-PNIPAM, trifunctional alkynyl-$(Cl)_2$ was prepared first and utilized as the ATRP initiator for the polymerization of the NIPAM monomer, thus affording PNIPAM-alkynyl-PNIPAM (Scheme 3c). The polymerization conditions were similar to those employed for the synthesis of alkynyl-PNIPAM, as described in the previous section. The overall DP of PNIPAM-alkynyl-PNIPAM was calculated to be 54, according to ^{1}H NMR spectroscopy results (Figure S3a in the Supporting Information). Thus, the alkynyl-functionalized polymer was denoted as $PNIPAM_{27}$-alkynyl-$PNIPAM_{27}$. The subsequent click reaction of $PNIPAM_{27}$-alkynyl-$PNIPAM_{27}$ with biotin azide afforded $PNIPAM_{27}$-biotin-$PNIPAM_{27}$. In the ^{1}H NMR spectrum, a new resonance signal at $\delta \approx 8.08$ ppm could be discerned, which verified the successful click reaction between biotin azide and alkynyl moiety (Figure S3b in the Supporting Information). GPC elution traces of $PNIPAM_{27}$-alkynyl-$PNIPAM_{27}$ and $PNIPAM_{27}$-biotin-$PNIPAM_{27}$ also revealed monomodal and symmetric peaks in both cases and the M_n of the latter shifted slightly from 6200 to 6400 (Figure S4 in the Supporting Information).

Finally, PEO-biotin-PNIPAM was prepared by the click reaction of PEO-alkynyl-PNIPAM with biotin azide (Scheme 3d). 3,5-Bis(propargyloxy)benzyl alcohol was prepared according to literature procedures.[20] Diblock copolymer with one single alkynyl moiety at the junction point, PEO-alkynyl-PNIPAM, was then synthesized in three steps. First, PEO-alkynyl-OH was synthesized by the click coupling reaction between PEO-N_3 and an excess of 3,5-bis(-propargyloxy)benzyl alcohol (20 equiv) under dilute conditions to assure that only one alkynyl group participated in the click reaction. The ^{1}H NMR spectrum of PEO-alkynyl-OH is shown in Figure 4a, together with signal assignments. Resonance signals characteristic of PEO and 3,5-bis(propargyloxy)benzyl alcohol can be clearly observed and the integral ratio of signal *f* to signal *g* is about 2:1; this confirmed the successful synthesis of PEO-alkynyl-OH. Compared with that of the PEO-N_3 precursor, the GPC trace of PEO-alkynyl-OH in DMF exhibited a slight shift towards higher with no tailing or shoulders (Figure 5A). This result further indicated that only one alkynyl group in 3,5-bis(propargyloxy)benzyl alcohol was consumed during the click reaction; otherwise, we would discern a shoulder peak corresponding to the coupled product, namely, PEO-OH-PEO.

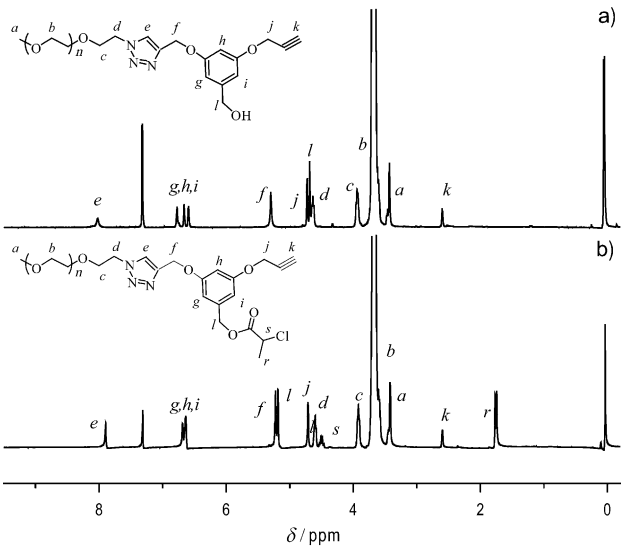

Figure 4. ^{1}H NMR spectra recorded in $CDCl_3$ for a) PEO_{45}-alkynyl-OH and b) PEO_{45}-alkynyl-Cl.

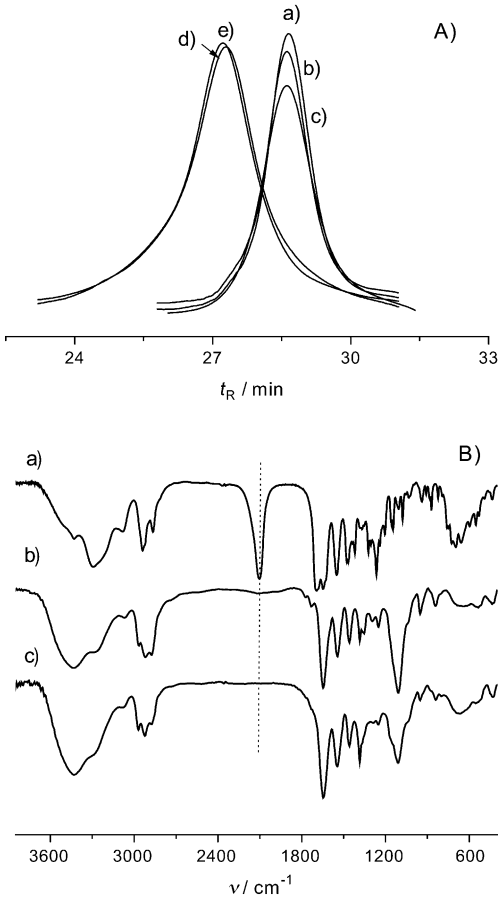

Figure 5. A) GPC traces recorded in DMF for a) PEO_{45}-N_3, b) PEO_{45}-alkynyl-OH, c) PEO_{45}-alkynyl-Cl, d) PEO_{45}-alkynyl-$PNIPAM_{45}$, and e) PEO_{45}-biotin-$PNIPAM_{45}$. B) FTIR spectra recorded for a) biotin azide, b) PEO_{45}-alkynyl-$PNIPAM_{45}$, and c) PEO_{45}-biotin-$PNIPAM_{45}$.

The hydroxyl functionality of PEO-alkynyl-OH was then treated with 2-chloropropionyl chloride to afford the ATRP macroinitiator, PEO-alkynyl-Cl. After the esterification reaction, the resonance signal of *l* shifted from $\delta = 4.69$ to 5.19 ppm (Figure 4b), and a new resonance signal ascribed to methyl protons (signal *r*) appeared at $\delta \approx 1.8$ ppm. The integral ratio of signal *j* to signal *r* was about 2:3, suggesting completion of the esterification reaction. The GPC elution trace of PEO-alkynyl-Cl revealed a narrow and symmetric peak with no tailing or shoulder at lower or higher MWs (Figure 5A).

Subsequently, PEO-alkynyl-PNIPAM was obtained by ATRP of the NIPAM monomer by using PEO-alkynyl-Cl as the macroinitiator. On the basis of the integral ratio of signal *f*, which was characteristic of PNIPAM, to signal *a*, which was characteristic of PEO sequences, the DP values of the PNIPAM block were estimated to be 45 (Figure 6a). Thus, the product was denoted as PEO_{45}-alkynyl-$PNIPAM_{45}$ (Table 1). Compared with the PEO-alkynyl-Cl precursor, the GPC trace of PEO-alkynyl-PNIPAM in DMF clearly shifted to higher MW, yielding M_w/M_n of 1.10 (Figure 5A). In the final step, PEO-alkynyl-PNIPAM was biotinylated by a click reaction with biotin azide. The ^{1}H NMR spectrum of PEO-biotin-PNIPAM is shown in Figure 6b. Compared with that of PEO-alkynyl-PNIPAM, the resonance signal ascribed to alkynyl moieties (signal *c*) almost disappeared and the signal ascribed to the proton in 1,3-triazole rings was considerably enhanced; this indicated the successful preparation of PEO-biotin-PNIPAM. Moreover, the GPC trace of PEO-biotin-PNIPAM in DMF exhibited a slight shift to higher MW associated with a narrow polydispersity of 1.10 (Figure 5A). The efficiency of the click reaction was further confirmed by FTIR analysis (Figure 5B), as evidenced by the complete disappearance of characteristic azide alkynyl moieties at about 2100 cm^{-1}).

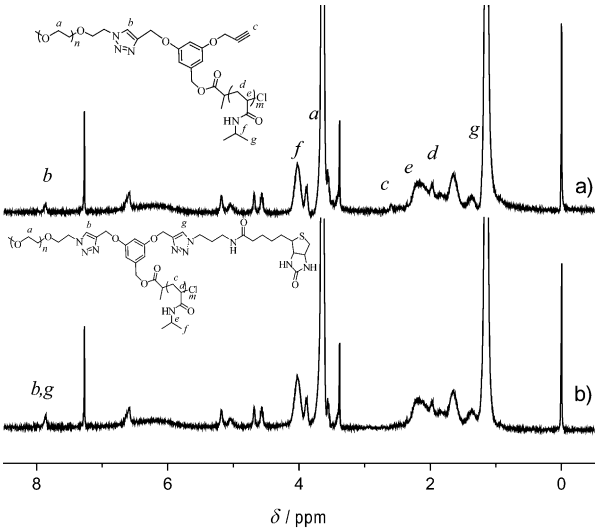

Figure 6. ^{1}H NMR spectra recorded in $CDCl_3$ for a) PEO_{45}-alkynyl-$PNIPAM_{45}$ and b) PEO_{45}-biotin-$PNIPAM_{45}$.

CHEMISTRY
AN ASIAN JOURNAL

Effects of Polymer MWs and Steric Hindrance on the Binding Numbers of Hybrid Polymer/Avidin Bioconjugates

Avidin is a glycoprotein consisting of four identical subunits and each subunit can strongly bind to one biotin with high affinity.[6] By taking advantage of this special interaction between avidin and biotin, we can facilely fabricate star polymers, star block copolymers, and heteroarm star copolymers starting from biotinylated polymers with the biotin functionality located at the chain terminal and chain middle of homopolymers and diblock copolymers (Table 2 and Scheme 2). A closer examination of the seven samples revealed that they could serve as a series of excellent systems for the investigation of polymer MW effects and steric hindrance effects on the binding affinity between avidin and biotinylated polymers. The binding numbers were then quantified by standard HABA/avidin assays.

The HABA/avidin reagent is quite sensitive and convenient for the spectroscopic examination of avidin/biotin binding events. In the absence of biotin or biotinylated polymers, HABA will specifically form a noncovalent molecular recognition complex with avidin with an association constant (K_a) of $7\times10^6\,M^{-1}$, and the complex exhibits a characteristic optical adsorption peak at about 500 nm. The addition of biotin or biotin derivatives to the HABA/avidin assay mixture will result in the displacement of HABA from the binding sites because the biotin/avidin K_a value is as high as $10^{15}\,M^{-1}$. This displacement event is also accompanied by a proportional decrease in the optical absorbance at 500 nm. Thus, the binding number of biotinylated polymer chains per avidin molecule can be facilely determined.

During the HABA/avidin assay, aqueous solutions of biotinylated polymers at predetermined concentrations were added dropwise to the HABA/avidin assay mixture (900 μL). The variation of optical absorbance at 500 nm was then recorded as a function of the amount of biotin-$PNIPAM_{19}$ aqueous solution added (Figure 7a). Upon addition of an aqueous solution of biotin-$PNIPAM_{19}$ (10–300 μL), the absorbance at 500 nm decreased almost linearly, indicating that biotin-$PNIPAM_{19}$ continuously binds avidin and replaces HABA from the initially formed HABA/avidin complex. Upon further addition of biotin-$PNIPAM_{19}$, the decrease of optical absorbance slowed down considerably, indicating that the binding of more biotin-$PNIPAM_{19}$ chains onto avidin was getting difficult. At later stages, the decrease could be mainly ascribed to the dilution effect. From the intersection point of the two lines, showing the changing trends at early and later stages of biotin-$PNIPAM_{19}$ addition (Figure 7a), the amount of biotin-$PNIPAM_{19}$ needed to maximally replace HABA molecules from the initially formed HABA/avidin complex can then be calculated. The binding number of biotin-$PNIPAM_{19}$ per avidin was thus determined to be about 3.3 (Table 2).

The above results indicated that the steric hindrance exerted by the covalently attached $PNIPAM_{19}$ chain almost did not inhibit the affinity binding between biotin-$PNIPAM_{19}$ and avidin, although the theoretical maximum

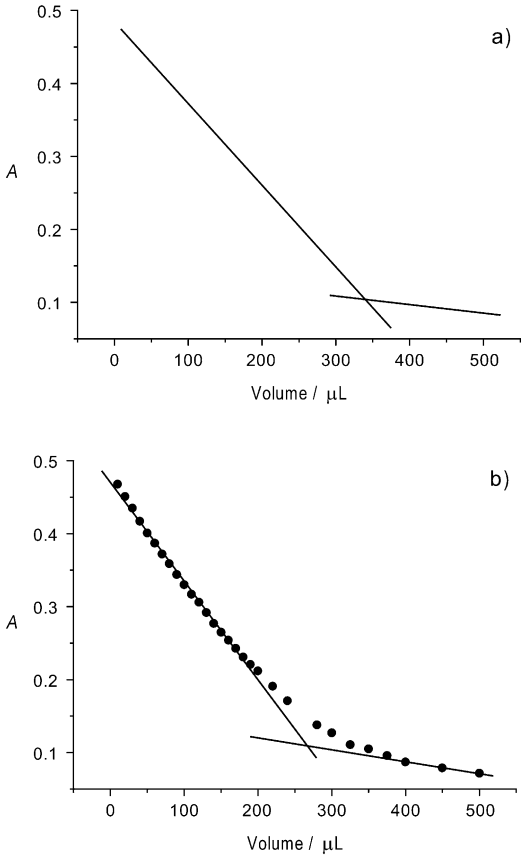

Figure 7. Variation of optical absorbance of HABA/avidin assay mixture upon titration with aqueous solutions of a) biotin-$PNIPAM_{19}$ and b) PEO_{45}-biotin-$PNIPAM_{45}$.

binding number is four. Another typical example is shown for PEO_{45}-biotin-$PNIPAM_{45}$, in which the biotin functionality is located at the junction point. From Figure 7b, we can tell that the trend of changes in optical absorbance with gradual addition of PEO_{45}-biotin-$PNIPAM_{45}$ is quite similar to that exhibited by biotin-$PNIPAM_{19}$. Apparently, the transition from quick decrease to slow decrease in optical absorbance occurs at much lower volume of PEO_{45}-biotin-$PNIPAM_{45}$ solution added than that for biotin-$PNIPAM_{19}$. Accordingly, the binding number of PEO_{45}-biotin-$PNIPAM_{45}$ chains per avidin was determined to be 2.2 (Table 2) and this clearly implied the steric hindrance effect. When the biotin moiety was located at the diblock junction, its binding with avidin will be opposed by the closely connected PEO and PNIPAM blocks. The above results partially confirmed our initial consideration. Also, note that based on the above description, heteroarm star copolymers have about 2.2 PEO and about 2.2 PNIPAM arms formed by binding between PEO_{45}-biotin-$PNIPAM_{45}$ and avidin.

Subsequently, the binding numbers for all biotinylated polymers during their conjugation with avidin were determined and the results are summarized in Table 2. For biotin-$PNIPAM_{19}$, biotin-$PNIPAM_{50}$, and biotin-$PNIPAM_{69}$-*b*-$PDMA_{65}$, the average binding numbers decreased from 3.3 to 2.9 to 1.9, respectively. This clearly suggested that the

higher polymer MWs, the lower binding affinity between avidin and biotin-terminated PNIPAM homopolymer or PNIPAM-*b*-PDMA diblock copolymer. A further comparison between the binding numbers of biotin-$PNIPAM_{50}$ and $PNIPAM_{27}$-biotin-$PNIPAM_{27}$, 2.9 and 1.9, respectively, revealed that the placement of the biotin functionality at the chain middle could dramatically decrease its binding tendency towards avidin because the two polymers possess similar chain lengths and only differ in the location of the biotin functionality within the chain. For PEO_{45}-biotin-$PNIPAM_{15}$ and PEO_{45}-biotin-$PNIPAM_{45}$, the biotin functionalities are both located at the diblock junction and the corresponding binding numbers are 2.5 and 2.2, respectively; this again reflected the effect of polymer MW of the biotinylated precursors on the binding process.

Moreover, the binding numbers of biotin-$PNIPAM_{50}$ and biotin-$PNIPAM_{19}$-*b*-$PDMA_8$ per avidin are both 2.9, which might be a coincidence and partially imply that PDMA chain conformations, noting that DMA is an *N*,*N*-dialkyl-substituted monomer, provide more steric hindrance to the avidin/biotin binding process than that exerted by the PNIPAM sequence. Another interesting comparison between $PNIPAM_{27}$-biotin-$PNIPAM_{27}$ (binding number 1.9) and PEO_{45}-biotin-$PNIPAM_{15}$ (binding number 2.5) further revealed that the PEO sequence exerted much lower steric hindrance to the molecular recognition event than that exerted by PNIPAM; this may be because the PEO chain conformation is quite flexible and contains no side groups.[17] We can thus deduce that for biotinylated PEO, PNIPAM, and PDMA of comparable chain lengths, the binding affinity with avidin decreases in the order of PEO > PNIPAM > PDMA owing to the steric hindrance effect of varying chain conformations and the absence or presence of side groups. Overall, the above results successfully interpreted the steric hindrance effects of polymer MWs, biotin location within the chain, and chain conformations of biotinylated polymers on their binding affinities, that is, binding number, with avidin. Note that the determination of binding numbers can also tell us the exact number of noncovalently grafted polymer arms per avidin within the supramolecular star polymers, star block copolymers, and heteroarm star copolymers (Schemes 1 and 2).

Finally, the availability of biotin moieties on biotinylated polymers for specific conjugation to surface-bound avidin and the binding process were further examined by using a diffractive optics technology (dotLab) system (Figure 8); this is a sensitive technique to monitor small changes in diffraction owing to binding events occurring at the surface of a sensor chip.[6e,26] As shown in Figure 8, a clear response is observed after the injection of aqueous solutions of either biotin-$PNIPAM_{19}$ or $PNIPAM_{27}$-biotin-$PNIPAM_{27}$. Most importantly, the signal increase retained to a large degree after washing. Qualitatively, we can also tell from Figure 8 that $PNIPAM_{27}$-biotin-$PNIPAM_{27}$ apparently exhibits a smaller response upon injection than that of biotin-$PNIPAM_{19}$, which suggested that the former exerts a larger steric hindrance effect during conjugation with avidin, and this is in qualitative agreement with the difference in the corresponding binding numbers (Table 2).

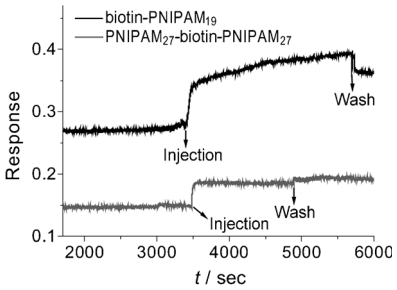

Figure 8. DotLab responses at the surface of an avidin-coated sensor chip upon injection of aqueous solutions of biotin-$PNIPAM_{19}$ and $PNIPAM_{27}$-biotin-$PNIPAM_{27}$.

Conclusion

A series of homopolymers and block copolymers site-specifically labeled with one single biotin functionality at the chain terminal, chain middle, or diblock junction point were synthesized by the combination of ATRP and click chemistry. By taking advantage of the specific noncovalent interaction between avidin and biotin moieties, polymer–protein bioconjugates with varying star-type topologies, including star polymers, star block copolymers, and heteroarm star polymers, were fabricated. The steric hindrance effects (polymer MW, location of biotin moiety within the chain, and polymer chain conformations) on the conjugation efficiency between biotinylated polymers and avidin were systematically explored. Standard avidin/HABA assays revealed that polymer MW and the location of biotin moiety within the polymer chain played crucial roles in the binding affinity, and the binding numbers varied from 3.3 to 1.9. For biotinylated polymers with similar chain architectures, but different MWs, those with larger MWs exhibited a lower binding affinity with avidin. For biotinylated polymers with comparable MWs, but different chain architecture, those with the biotin functionality located at the chain middle or diblock junction point possessed higher steric hindrance during conjugation with avidin than those of biotin-terminated polymers. Finally, for biotinylated PEO, PNIPAM, and PDMA of comparable chain lengths, the binding affinity with avidin decreased in the order of PEO > PNIPAM > PDMA through the steric hindrance effect as a result of different chain conformations and the absence or presence of side groups.

Acknowledgements

The financial support from the National Natural Scientific Foundation of China (NNSFC) Project (20874092, 91027026, and 51033005) and the Fundamental Research Funds for the Central Universities is gratefully acknowledged.

[1] a) S. F. M. van Dongen, H. P. M. de Hoog, R. J. R. W. Peters, M. Nallani, R. J. M. Nolte, J. C. M. van Hest, *Chem. Rev.* **2009**, *109*, 6212–6274; b) I. C. Reynhout, J. J. L. M. Cornelissen, R. J. M. Nolte, *Acc. Chem. Res.* **2009**, *42*, 681–692; c) R. Duncan, *Nat. Rev. Drug Discovery* **2003**, *2*, 347–360; d) Z. L. Ding, R. B. Fong, C. J. Long, P. S. Stayton, A. S. Hoffman, *Nature* **2001**, *411*, 59–62; e) L. A. Canalle, D. W. P. M. Lowik, J. C. M. van Hest, *Chem. Soc. Rev.* **2010**, *39*, 329–353; f) A. K. Shakya, H. Sami, A. Srivastava, A. Kumar, *Prog. Polym. Sci.* **2010**, *35*, 459–486; g) H. G. Börner, *Macromol. Chem. Phys.* **2007**, *208*, 124–130; h) J. M. Hu, S. Y. Liu, *Macromolecules* **2010**, *43*, 8315–8330.

[2] M. J. Roberts, M. D. Bentley, J. M. Harris, *Adv. Drug Delivery Rev.* **2002**, *54*, 459–476.

[3] a) P. De, M. Li, S. R. Gondi, B. S. Sumerlin, *J. Am. Chem. Soc.* **2008**, *130*, 11288–11289; b) M. E. B. Smith, F. F. Schumacher, C. P. Ryan, L. M. Tedaldi, D. Papaioannou, G. Waksman, S. Caddick, J. R. Baker, *J. Am. Chem. Soc.* **2010**, *132*, 1960–1965; c) B. Le Droumaguet, G. Mantovani, D. M. Haddleton, K. Velonia, *J. Mater. Chem.* **2007**, *17*, 1916–1922; d) K. L. Heredia, G. N. Grover, L. Tao, H. D. Maynard, *Macromolecules* **2009**, *42*, 2360–2367.

[4] a) Q. Wang, T. R. Chan, R. Hilgraf, V. V. Fokin, K. B. Sharpless, M. G. Finn, *J. Am. Chem. Soc.* **2003**, *125*, 3192–3193; b) M. van Dijk, D. T. S. Rijkers, R. M. J. Liskamp, C. F. van Nostrum, W. E. Hennink, *Bioconjugate Chem.* **2009**, *20*, 2001–2016; c) B. Le Droumaguet, K. Velonia, *Macromol. Rapid Commun.* **2008**, *29*, 1073–1089; d) A. J. T. Dirks, S. S. van Berkel, N. S. Hatzakis, J. A. Opsteen, F. L. van Delft, J. J. L. M. Cornelissen, A. E. Rowan, J. C. M. van Hest, F. P. J. T. Rutjes, R. J. M. Nolte, *Chem. Commun.* **2005**, 4172–4174.

[5] a) L. Tao, J. Q. Liu, T. P. Davis, *Biomacromolecules* **2009**, *10*, 2847–2851; b) J. Q. Liu, V. Bulmus, D. L. Herlambang, C. Barner-Kowollik, M. H. Stenzel, T. P. Davis, *Angew. Chem.* **2007**, *119*, 3159–3163; *Angew. Chem. Int. Ed.* **2007**, *46*, 3099–3103; c) D. Bontempo, K. L. Heredia, B. A. Fish, H. D. Maynard, *J. Am. Chem. Soc.* **2004**, *126*, 15372–15373.

[6] a) C. A. Lackey, N. Murthy, O. W. Press, D. A. Tirrell, A. S. Hoffman, P. S. Stayton, *Bioconjugate Chem.* **1999**, *10*, 401–405; b) S. Kulkarni, C. Schilli, A. H. E. Muller, A. S. Hoffman, P. S. Stayton, *Bioconjugate Chem.* **2004**, *15*, 747–753; c) J. K. Oh, D. J. Siegwart, H. I. Lee, G. Sherwood, L. Peteanu, J. O. Hollinger, K. Kataoka, K. Matyjaszewski, *J. Am. Chem. Soc.* **2007**, *129*, 5939–5945; d) X. Z. Jiang, S. Y. Liu, R. Narain, *Langmuir* **2009**, *25*, 13344–13350; e) A. Housni, H. J. Cai, S. Y. Liu, R. Narain, *Langmuir* **2007**, *23*, 5056–5061.

[7] a) I. C. Reynhout, J. J. L. M. Cornelissen, R. J. M. Nolte, *J. Am. Chem. Soc.* **2007**, *129*, 2327–2332; b) X. J. Wan, S. Y. Liu, *Macromol. Rapid Commun.* **2010**, *31*, 2070–2076.

[8] a) Y. Koshi, E. Nakata, M. Miyagawa, S. Tsukiji, T. Ogawa, I. Hamachi, *J. Am. Chem. Soc.* **2008**, *130*, 245–251; b) M. L. Wolfenden, M. J. Cloninger, *J. Am. Chem. Soc.* **2005**, *127*, 12168–12169.

[9] a) I. Hwang, K. Baek, M. Jung, Y. Kim, K. M. Park, D. W. Lee, N. Selvapalam, K. Kim, *J. Am. Chem. Soc.* **2007**, *129*, 4170–4171.

[10] a) J. Nicolas, G. Mantovani, D. M. Haddleton, *Macromol. Rapid Commun.* **2007**, *28*, 1083–1111; b) Y. A. Lin, J. M. Chalker, B. G. Davis, *J. Am. Chem. Soc.* **2010**, *132*, 16805–16811; c) H. M. Li, A. P. Bapat, M. Li, B. S. Sumerlin, *Polym. Chem.* **2011**, *2*, 323–327; d) M. Li, P. De, H. M. Li, B. S. Sumerlin, *Polym. Chem.* **2010**, *1*, 854–859; e) V. Bulmus, *Polym. Chem.* **2011**, *2*, 1463–1472; f) X. Huang, C. Boyer, T. P. Davis, V. Bulmus, *Polym. Chem.* **2011**, *2*, 1505–1512; g) M. Chenal, C. Boursier, Y. Guillaneuf, M. Taverna, P. Couvreur, J. Nicolas, *Polym. Chem.* **2011**, *2*, 1523–1530; h) H. M. Li, M. Li, X. Yu, A. P. Bapat, B. S. Sumerlin, *Polym. Chem.* **2011**, *2*, 1531–1535; i) M. Li, H. M. Li, P. De, B. S. Sumerlin, *Macromol. Rapid Commun.* **2011**, *32*, 354–359; j) M. Li, P. De, S. R. Gondi, B. S. Sumerlin, *Macromol. Rapid Commun.* **2008**, *29*, 1172–1176; k) H. Liu, X. Z. Jiang, J. Fan, G. H. Wang, S. Y. Liu, *Macromolecules* **2007**, *40*, 9074–9083.

[11] a) J. C. Peeler, B. F. Woodman, S. Averick, S. J. Miyake-Stoner, A. L. Stokes, K. R. Hess, K. Matyjaszewski, R. A. Mehl, *J. Am. Chem. Soc.* **2010**, *132*, 13575–13577; b) B. Le Droumaguet, K. Velonia, *Angew. Chem.* **2008**, *120*, 6359–6362; *Angew. Chem. Int. Ed.* **2008**, *47*, 6263–6266.

[12] a) C. Boyer, V. Bulmus, J. Q. Liu, T. P. Davis, M. H. Stenzel, C. Barner-Kowollik, *J. Am. Chem. Soc.* **2007**, *129*, 7145–7154.

[13] a) P. S. Stayton, T. Shimoboji, C. Long, A. Chilkoti, G. H. Chen, J. M. Harris, A. S. Hoffman, *Nature* **1995**, *378*, 472–474; b) J. M. Hannink, J. J. L. M. Cornelissen, J. A. Farrera, P. Foubert, F. C. De Schryver, N. A. J. M. Sommerdijk, R. J. M. Nolte, *Angew. Chem.* **2001**, *113*, 4868–4870; *Angew. Chem. Int. Ed.* **2001**, *40*, 4732–4734; c) J. Jin, D. X. Wu, P. C. Sun, L. Liu, H. Y. Zhao, *Macromolecules* **2011**, *44*, 2016–2024; d) W. Shi, S. Dolai, S. Averick, S. S. Fernando, J. A. Saltos, W. L′Amoreaux, P. Banerjee, K. Raja, *Bioconjugate Chem.* **2009**, *20*, 1595–1601.

[14] a) D. Bontempo, H. D. Maynard, *J. Am. Chem. Soc.* **2005**, *127*, 6508–6509; b) D. Bontempo, R. C. Li, T. Ly, C. E. Brubaker, H. D. Maynard, *Chem. Commun.* **2005**, 4702–4704.

[15] a) L. Tao, J. Geng, G. J. Chen, Y. J. Xu, V. Ladmiral, G. Mantovani, D. M. Haddleton, *Chem. Commun.* **2007**, 3441–3443; b) F. Wurm, J. Klos, H. J. Rader, H. Frey, *J. Am. Chem. Soc.* **2009**, *131*, 7954–7955.

[16] a) K. Kaiser, M. Marek, T. Haselgrubler, H. Schindler, H. J. Gruber, *Bioconjugate Chem.* **1997**, *8*, 545–551; b) M. Marek, K. Kaiser, H. J. Gruber, *Bioconjugate Chem.* **1997**, *8*, 560–566.

[17] S. Ke, J. C. Wright, G. S. Kwon, *Bioconjugate Chem.* **2007**, *18*, 2109–2114.

[18] a) C. J. Huang, F. C. Chang, *Macromolecules* **2009**, *42*, 5155–5166; b) X. Z. Jiang, J. Y. Zhang, Y. M. Zhou, J. Xu, S. Y. Liu, *J. Polym. Sci. Part A* **2008**, *46*, 860–871.

[19] M. Ciampolini, N. Nardi, *Inorg. Chem.* **1966**, *5*, 41–44.

[20] Y. F. Zhang, H. Liu, H. F. Dong, C. H. Li, S. Y. Liu, *J. Polym. Sci. Part A* **2009**, *47*, 1636–1650.

[21] Y. F. Zhang, C. H. Li, S. Y. Liu, *J. Polym. Sci. Part A* **2009**, *47*, 3066–3077.

[22] a) J. Xu, J. Ye, S. Y. Liu, *Macromolecules* **2007**, *40*, 9103–9110; b) H. X. Xu, J. Xu, Z. Y. Zhu, H. W. Liu, S. Y. Liu, *Macromolecules* **2006**, *39*, 8451–8455; c) D. Wang, J. Yin, Z. Y. Zhu, Z. S. Ge, H. W. Liu, S. P. Armes, S. Y. Liu, *Macromolecules* **2006**, *39*, 7378–7385.

[23] X. J. Wan, S. Y. Liu, *J. Mater. Chem.* **2011**, *21*, 10321–10329.

[24] a) Y. Xia, X. C. Yin, N. A. D. Burke, H. D. H. Stover, *Macromolecules* **2005**, *38*, 5937–5943; b) X. C. Yin, H. D. H. Stover, *Macromolecules* **2005**, *38*, 2109–2115.

[25] T. L. Hsu, S. R. Hanson, K. Kishikawa, S. K. Wang, M. Sawa, C. H. Wong, *Proc. Natl. Acad. Sci. USA* **2007**, *104*, 2614–2619.

[26] X. Z. Jiang, A. Housni, G. Gody, P. Boullanger, M. T. Charreyre, T. Delair, R. Narain, *Bioconjugate Chem.* **2010**, *21*, 521–530.

Received: May 27, 2011
Published online: September 2, 2011

